

REPORT DOCUMENTATION PAGE

Form Approved OMB NO. 0704-0188

The public reporting burden for this collection of information is estimated to average 1 hour per response, including the time for reviewing instructions, searching existing data sources, gathering and maintaining the data needed, and completing and reviewing the collection of information. Send comments regarding this burden estimate or any other aspect of this collection of information, including suggestions for reducing this burden, to Washington Headquarters Services, Directorate for Information Operations and Reports, 1215 Jefferson Davis Highway, Suite 1204, Arlington VA, 22202-4302. Respondents should be aware that notwithstanding any other provision of law, no person shall be subject to any penalty for failing to comply with a collection of information if it does not display a currently valid OMB control number.

PLEASE DO NOT RETURN YOUR FORM TO THE ABOVE ADDRESS.

1. REPORT DATE (DD-MM-YYYY)	2. REPORT TYPE	3. DATES COVERED (From - To)	
	New Reprint	-	
4. TITLE AND SUBTITLE Polarity Control and growth of lateral polarity structures in AlN		5a. CONTRACT NUMBER	
		5b. GRANT NUMBER W911NF-04-D-0003	
		5c. PROGRAM ELEMENT NUMBER 611102	
6. AUTHORS Ronny Kirste, Seiji Mita, Lindsay Hussey, Marc Hoffmann, Wei Guo, Isaac Bryan, Zachary Bryan, James Tweedie, Jinqiao Xie, Michael Gerhold, Ramon Collazo, Zlatko Sitar		5d. PROJECT NUMBER	
		5e. TASK NUMBER	
		5f. WORK UNIT NUMBER	
7. PERFORMING ORGANIZATION NAMES AND ADDRESSES North Carolina State University Research Administration 2701 Sullivan Drive, Suite 240 Raleigh, NC 27695 -7514		8. PERFORMING ORGANIZATION REPORT NUMBER	
9. SPONSORING/MONITORING AGENCY NAME(S) AND ADDRESS(ES) U.S. Army Research Office P.O. Box 12211 Research Triangle Park, NC 27709-2211		10. SPONSOR/MONITOR'S ACRONYM(S) ARO	
		11. SPONSOR/MONITOR'S REPORT NUMBER(S) 57365-EL-SR.2	
12. DISTRIBUTION AVAILABILITY STATEMENT Approved for public release; distribution is unlimited.			
13. SUPPLEMENTARY NOTES The views, opinions and/or findings contained in this report are those of the author(s) and should not be construed as an official Department of the Army position, policy or decision, unless so designated by other documentation.			
14. ABSTRACT The control of the polarity of metalorganic chemical vapor deposition grown AlN on sapphire is demonstrated. Al-polar and N-polar AlN is grown side-by-side yielding a lateral polarity structure. Scanning electron microscopy measurements reveal a smooth surface for the Al-polar and a relatively rough surface for the N-polar AlN domains. Transmission electron microscopy shows mixed edge-screw type dislocations with polarity-dependent dislocation bending. Raman			
15. SUBJECT TERMS AlN, lateral polar structures, metal organic chemical vapor deposition			
16. SECURITY CLASSIFICATION OF: a. REPORT UU		17. LIMITATION OF ABSTRACT b. ABSTRACT UU c. THIS PAGE UU	15. NUMBER OF PAGES 19a. NAME OF RESPONSIBLE PERSON Michael Gerhold 19b. TELEPHONE NUMBER 919-549-4357

Report Title

Polarity Control and growth of lateral polarity structures in AlN

ABSTRACT

The control of the polarity of metalorganic chemical vapor deposition grown AlN on sapphire is demonstrated. Al-polar and N-polar AlN is grown side-by-side yielding a lateral polarity structure. Scanning electron microscopy measurements reveal a smooth surface for the Al-polar and a relatively rough surface for the N-polar AlN domains. Transmission electron microscopy shows mixed edge-screw type dislocations with polarity-dependent dislocation bending. Raman spectroscopy reveals compressively strained Al-polar and relaxed N-polar domains. The near band edge luminescence consists of free and bound excitons which are broadened for the Al-polar AlN. Relaxation, better optical quality, and dislocation bending in the N-polar domains are explained by the columnar growth mode. VC 2013 AIP Publishing LLC.

REPORT DOCUMENTATION PAGE (SF298)
(Continuation Sheet)

Continuation for Block 13

ARO Report Number 57365.2-EL-SR
Polarity Control and growth of lateral polarity stru ...

Block 13: Supplementary Note

© 2013 . Published in Appl. Phys. Lett., Vol. Ed. 0 102, (1) (2013), (, (1). DoD Components reserve a royalty-free, nonexclusive and irrevocable right to reproduce, publish, or otherwise use the work for Federal purposes, and to authroize others to do so (DODGARS §32.36). The views, opinions and/or findings contained in this report are those of the author(s) and should not be construed as an official Department of the Army position, policy or decision, unless so designated by other documentation.

Approved for public release; distribution is unlimited.

Polarity control and growth of lateral polarity structures in AlN

Ronny Kirste,¹ Seiji Mita,² Lindsay Hussey,¹ Marc P. Hoffmann,¹ Wei Guo,¹ Isaac Bryan,¹ Zachary Bryan,¹ James Tweedie,¹ Jinqiao Xie,² Michael Gerhold,³ Ramón Collazo,¹ and Zlatko Sitar¹

¹Department of Materials Science and Engineering, North Carolina State University, Raleigh, North Carolina 27695-7919, USA

²HexaTech, Inc., 991 Aviation Pkwy., Suite 800, Morrisville, North Carolina 27560, USA

³Engineering Science Directorate, Army Research Office, P.O. Box 12211, Research Triangle Park, North Carolina 27703, USA

(Received 6 April 2013; accepted 18 April 2013; published online 10 May 2013)

The control of the polarity of metalorganic chemical vapor deposition grown AlN on sapphire is demonstrated. Al-polar and N-polar AlN is grown side-by-side yielding a lateral polarity structure. Scanning electron microscopy measurements reveal a smooth surface for the Al-polar and a relatively rough surface for the N-polar AlN domains. Transmission electron microscopy shows mixed edge-screw type dislocations with polarity-dependent dislocation bending. Raman spectroscopy reveals compressively strained Al-polar and relaxed N-polar domains. The near band edge luminescence consists of free and bound excitons which are broadened for the Al-polar AlN. Relaxation, better optical quality, and dislocation bending in the N-polar domains are explained by the columnar growth mode. © 2013 AIP Publishing LLC. [<http://dx.doi.org/10.1063/1.4804575>]

AlN is an interesting material for numerous optical and electronic applications. Most devices that have been demonstrated on AlN have been grown on the Al-polar face since this anionic polar orientation, comparable to GaN, InN, or ZnO, is characterized by low unwanted impurity incorporation, which eases doping possibilities.^{1,2} However, especially for electronic applications and sensors, N-polar AlN may have advantages.^{3,4} In addition, if the N-polar AlN is grown side-by-side to the Al-polar material, a lateral polarity structure can be fabricated. Such lateral control of the polarity could ultimately lead to a new class of devices similar to those predicted for GaN.⁵ This could include high-power and high-frequency field effect transistors, efficient ultraviolet (UV) light emitting diodes, or UV-laser light generation via frequency doubling.⁶ A few prerequisites are lateral control on the micrometer or even nanometer length-scale, growth of high quality AlN layers of either polarity, growth rate control of adjacent domains, and sharp interfaces between the domains of opposite polarities.

In this paper, we demonstrate simultaneous growth of Al- and N-polar AlN on sapphire using a patterned low temperature (LT)-AlN buffer layer, thus yielding a lateral polarity structure with a controlled domain size down to 5 μm. These lateral polarity structures were investigated using scanning electron microscopy (SEM), transmission electron microscopy (TEM), Raman spectroscopy, and photoluminescence measurements. In contrast to the Al-polar domains, which are found to be grown fully coalesced, a columnar growth mode of the N-polar films with partial coalescence is observed. This variation in the growth mechanism is established as the origin of an observed decreased strain, dislocation bending, and better optical quality of the N-polar domains.

In order to control the polarity, a LT-buffer layer was grown at 650 °C. The buffer layer was patterned by reactive-ion etching. Subsequent growth of high temperature (1250 °C) AlN resulted in Al-polar domains in areas with an

underlying LT-AlN layer and N-polar AlN where the buffer layer was removed, similar to the polarity control schemes already demonstrated for GaN.⁷ Following the patterning, 600 nm thick AlN was grown by metalorganic chemical vapor deposition at 80 Torr in a hydrogen atmosphere with a NH₃ and trimethylaluminium mass flow of 4.46 mmol/min and 21 μmol/min, respectively. Domain sizes ranging from 5 μm up to 5 mm were achieved for both domain types, as determined by the mask feature size.

KOH etching was performed at 70 °C for 1 min to verify the different polarities of the patterned AlN film.⁸ Figure 1 shows an optical micrograph of the 50 μm wide stripes with periodically oriented Al-polar and N-polar AlN stripes before (top) and after (bottom) KOH etching. While no etching is observed on the Al-polar domains, a complete removal of the N-polar film is observed. This finding is consistent

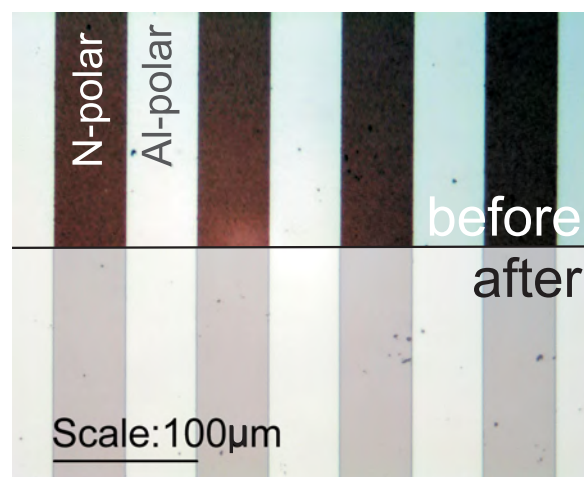


FIG. 1. Optical image of the surface of an AlN layer with stripes of alternating polarity before (top) and after (bottom) KOH-etching. Due to the polarity-dependent etching rate of AlN, the Al-polar surface did not undergo change under the etching while the N-polar film was removed completely.

with the etching rate of approximately 1400 nm/min for the N-polar AlN versus 2 nm/min for the Al-polar material and proves a successful side-by-side growth of polarity-pure N-polar and Al-polar AlN domains.

The darker color of the N-polar domains in the optical image in Figure 1 corresponds to a different surface morphology and strong scattering on the N-polar surface. SEM images were recorded in order to investigate the surface morphology and the layer structure in detail. A typical SEM image of the region around the inversion domain boundary between the two polarities is shown in Figure 2. In accordance with results known from GaN, the III-polar layer is fully coalesced and exhibits a smooth surface with few defects.⁹ Atomic force microscopy reveals step flow morphology with root mean square (RMS) values of 0.3 nm on a $5 \times 5 \mu\text{m}$ area scan (not shown). In contrast, the N-polar film exhibits a columnar structure that is coalesced near the bottom. X-ray diffraction (XRD) measurement of the N- and Al-polar regions revealed a comparable full width at half maximum of the (002) and (102) peaks of 300–400 arc sec and 850 arc sec, respectively, indicating a low mosaicity of both types of domains. Thus, the columnar structure observed for the N-polar domains seems to be well ordered and aligned. The changed layer structure of the N-polar film is interpreted as a change of the growth mode. A two-dimensional growth mode is expected for the Al-polar film, while N-polar AlN tends to grow in a 3D columnar morphology leading to a rough surface with RMS values around 15 nm.^{10,11} The boundary between the Al- and N-polar AlN is well defined. Even for the smallest feature sizes ($5 \mu\text{m}$), very sharp interfaces and well-defined domains were observed, indicating that even smaller features sizes are possible in the future, which is important for applications of the AlN lateral polarity structures. Cross-sectional SEM micrographs revealed a height difference between the two films of opposite polarity of 10–30 nm, which is mainly assigned to the thickness of the underlying AlN-buffer layer. This finding highlights an equal growth rate of the Al-polar and

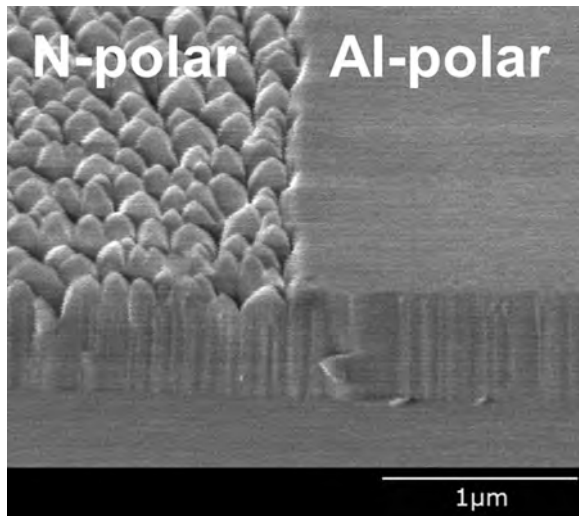


FIG. 2. SEM micrograph (60° tilt) of a 600 nm AlN layer with areas of opposite polarity. The N-polar domain consists of multiple columnar features that are coalesced at the bottom. In contrast the Al-polar film is fully coalesced with a smooth surface.

N-polar AlN for typical metalorganic chemical vapor deposition (MOCVD) conditions, which is in contrast to earlier findings in GaN.^{5,9}

TEM cross-section samples were prepared using a FEI 3D Quanta FEG Focused Ion Beam system. Transmission electron microscopy was performed with a JEOL 2000FX operating at 200 kV. Figure 3 displays bright field TEM images of a lateral polarity boundary with the g-vector chosen parallel (top) and perpendicular (bottom) to the c-axis. As observed with SEM, the N-polar domain consists of many “nano”-columns that are well coalesced within the first 300–400 nm and partially separated towards the surface. The diameter of the columns is estimated to 100–200 nm. Within the N-polar region, a few V-like structures are observed (white arrows). Similar structures were previously observed by Jasinski *et al.* and Romano *et al.* in AlN and GaN and were identified as inversion domains (IDs) using KOH etching and convergent beam electron diffraction.^{12,13} This identification as inversion domains was confirmed by scanning tunneling electron microscopy measurements which clearly revealed a polarity change to the Al-polar orientation in the N-polar domain (not shown). The observed IDs grew under an angle of approximately 4° which is comparable to the angle observed by Jasinski *et al.* All IDBs are formed on top of voids in the sapphire with diameters of 10 nm (Figure 3, white circles). The origin of these voids has been previously attributed to the decomposition of sapphire due to the high temperatures at which the samples were grown.¹⁴ Interestingly, similar voids are not only observed underneath the N-polar domain region but also in the Al-polar domain. However, the voids have no influence on the growth of Al-polar domains. In addition to the voids and IDs, dislocations are observed. Both polar domains contain a low density of screw-type dislocations; most dislocations are of mixed type. The dislocation density is observed to be around $1 \times 10^{10} \text{ cm}^{-2}$ and is similar in both the Al- and N-polar domains. Both values are comparable to

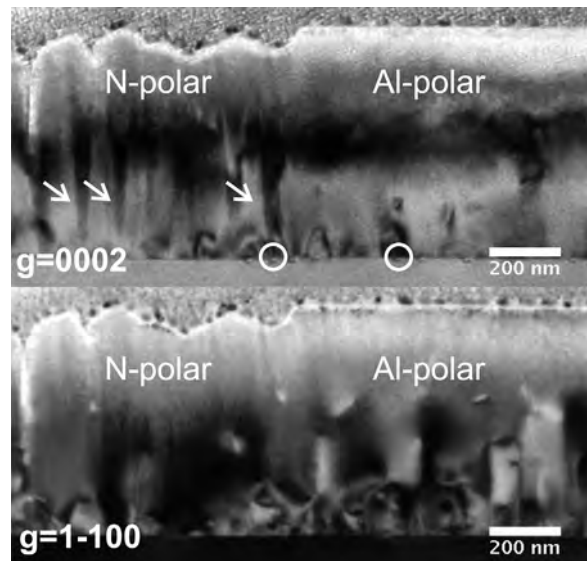


FIG. 3. Bright field TEM image of the AlN layer in the region of the inversion domain boundary with the N-polar film (left) and the Al-polar film (right) recorded with the g vector chosen parallel (top) and perpendicular (bottom) to the c-axis. Arrows indicate inversion domain boundaries in N-polar AlN, and circles mark positions of voids in the sapphire substrate.

typical dislocation densities previously reported for N- and Al-polar AlN on sapphire.^{10,15} For the N-polar films, most dislocations undergo bending near the sapphire interface leading to a strongly reduced dislocation density at the film surface. In contrast, in the Al-polar AlN, the bending is not as pronounced. This difference is expected to arise from the different growth modes between the two polar domains. The N-polar domains columnar growth mode leads to lower strains as relaxation occurs through surface roughening and 3D growth, which allows for dislocation bending near the free surfaces offered by the columnar geometry.

In order to estimate the strain in the Al- and N-polar domains, Raman spectroscopy investigations were performed. Figure 4 shows Raman spectra recorded for both domains. Due to the limited lateral resolution of micro Raman spectroscopy, no spectra could be obtained from the inversion domain boundary.⁹ Spectra were recorded at room temperature in z(xx)z geometry.¹⁶ The non-polar E₂(high) mode can be used to estimate the strain in the layers if the position of strain-free AlN at 656 cm⁻¹ is considered.¹⁶ The position of the E₂(high) mode in the Al-polar domain is 653.3 cm⁻¹ indicating a tensile strain around 0.6 GPa and 657.3 cm⁻¹ in the N-polar region indicating a small compressive strain around 0.1 GPa, respectively.¹⁷ This finding is supported by the XRD measurements and confirms the conclusions made from the TEM analysis. Due to the large lattice mismatch between the AlN and sapphire, the fully coalesced Al-polar layer is highly strained with an increased dislocation density leading to only partial relaxation. In contrast, the N-polar AlN exhibits only a relatively small compressive strain, which is related to the 3D growth. In addition to the E₂(high) mode, the A₁(LO) mode is allowed in the applied Raman geometry. A slight shift and broadening is observed if the signals from the Al- and N-polar domains are compared. However, the shift as well as the broadening are negligible and can be simply explained with the difference in the strain level.¹⁸

Low temperature (5 K) photoluminescence spectra were recorded using an ArF (193 nm) laser, a 0.75 m monochromator, and a charged coupled device detector. Two representative spectra of the near band edge luminescence for the two domain

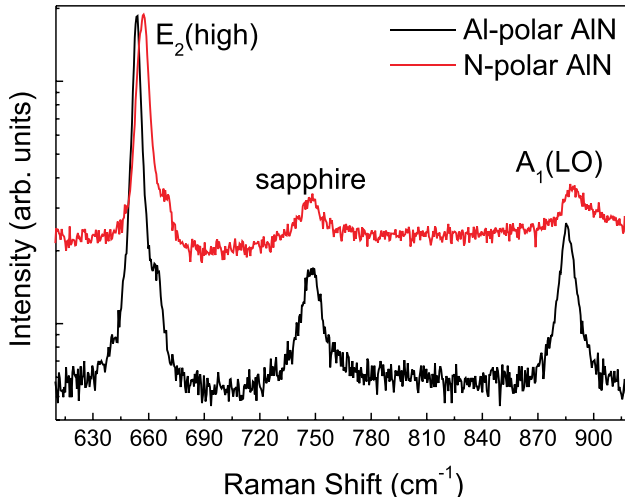


FIG. 4. Room temperature Raman spectra of the Al-polar and N-polar domains recorded in z(xx)z geometry.

types are shown in Figure 5(b). In the N-polar domains, the main peaks are identified as the free A-exciton (FX_A) around 6.034 eV, a silicon related donor bound exciton (D⁰X) at 6.012, and their corresponding phonon replicas around 5.92 eV.^{19,20} This assignment is confirmed by the energy value as well as temperature dependent photoluminescence measurements. Interestingly, the free exciton emission is dominating the spectrum even at low temperatures. This is not expected as all excitons are expected to be bound to impurities. However, similar observations were made for AlN/sapphire before but not for homoepitaxially grown layers, and more detailed investigations will be needed in the future to explain this unexpected observation.²¹ The Al-polar domains have the same emission lines as the N-polar domains, but they are considerably shifted to higher energies and broadened (e.g., FX_A from 14.3 meV to 22.3 meV) suggesting a higher optical quality of the N-polar domains. Such broadening would be typically explained by a decreased crystal quality of the Al-polar film, which may lead to increased carrier scattering at structural defects, and, thus, decreased carrier lifetimes. However, XRD, TEM, and Raman do not support such conclusion as they indicated comparable crystal quality. It may be argued that the increased optical quality of the N-polar film is related to the columnar structure, but further investigations will be necessary to clarify this conclusion. Following the results from Pantha *et al.*, the shift to higher energies is consistent with the compressive strain as observed by Raman spectroscopy.²² Finally, the deep defect luminescence shows a one order of magnitude increase of the intensity of the emissions at 3.5 eV, 3.2 eV, and 4.4–4.7 eV for the N-polar AlN (Figure 5(a)), which were assigned to silicon, oxygen, and Al-vacancies, respectively.^{23,24} This indicates that comparable to GaN or InN, increased point defect incorporation occurs on the anion side of polar AlN or increased incorporation of non-radiative defects occurs on the cation side of AlN.²⁵

In conclusion, AlN-based lateral polarity structures were grown by MOCVD on sapphire substrates. Control of the polarity was achieved by using a patterned low temperature AlN buffer layer: Al-polar domains grew on top of the LT

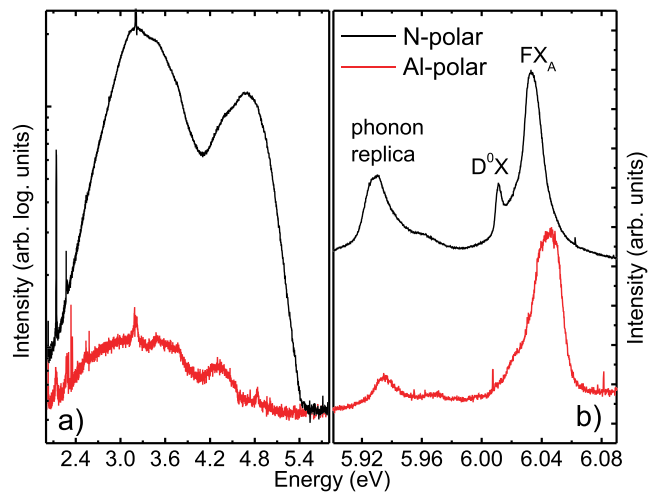


FIG. 5. Low temperature (5 K) photoluminescence spectra of the Al-polar and N-polar AlN film in the region of deep defect luminescence (a) and the free and bound excitons (b). Note the different scaling of the y-axis of the graphs. For clarity, the near band edge luminescence signal was normalized and shifted vertically.

buffer while N-polar domains grew on bare sapphire. SEM and TEM images revealed a columnar appearance of the N-polar domains, suggesting a 3D growth mode. This growth mode is responsible for the decreased strain and better optical quality of the N-polar domains. The results presented within this work will allow for a new class of AlN-based lateral polarity devices similar to those proposed for GaN.

This work was supported in part by the Army Research Laboratory (Contract No. W911NF-04-D-0003), William Clark program monitor, and NSF under Contract No. DMR-1108071. We thank Professor Axel Hoffmann of TU Berlin for the support in the Raman spectroscopy measurements.

- ¹J. Li, Z. Y. Fan, R. Dahal, M. L. Nakarmi, J. Y. Lin, and H. X. Jiang, *Appl. Phys. Lett.* **89**(21), 213510–213513 (2006).
- ²N. Dietz, M. Alevli, R. Atalay, G. Durkaya, R. Collazo, J. Tweedie, S. Mita, and Z. Sitar, *Appl. Phys. Lett.* **92**(4), 041911–041913 (2008).
- ³S. Rajan, A. Chini, M. H. Wong, J. S. Speck, and U. K. Mishra, *J. Appl. Phys.* **102**(4), 044501–044506 (2007).
- ⁴H. Kim, J.-H. Ryoo, R. D. Dupuis, S.-N. Lee, Y. Park, J.-W. Jeon, and T.-Y. Seong, *Appl. Phys. Lett.* **93**(19), 192106 (2008).
- ⁵M. Stutzmann, O. Ambacher, M. Eickhoff, U. Karrer, A. L. Pimenta, R. Neuberger, J. Schalwig, R. Dimitrov, P. Schuck, and R. Grober, *Phys. Status Solidi B* **228**(2), 505–512 (2001).
- ⁶A. Chowdhury, H. M. Ng, M. Bhardwaj, and N. G. Weimann, *Appl. Phys. Lett.* **83**(6), 1077–1079 (2003).
- ⁷F. Liu, R. Collazo, S. Mita, Z. Sitar, G. Duscher, and S. J. Pennycook, *Appl. Phys. Lett.* **91**(20), 203115 (2007).
- ⁸W. Guo, J. Xie, C. Akouala, S. Mita, A. Rice, J. Tweedie, I. Bryan, R. Collazo, and Z. Sitar, *J. Cryst. Growth* **366**, 20–25 (2013).
- ⁹R. Kirste, R. Collazo, G. Callsen, M. R. Wagner, T. Kure, J. S. Reparaz, S. Mita, J. Xie, A. Rice, J. Tweedie, Z. Sitar, and A. Hoffmann, *J. Appl. Phys.* **110**(9), 093503–093509 (2011).
- ¹⁰J. Bai, M. Dudley, W. H. Sun, H. M. Wang, and M. A. Khan, *Appl. Phys. Lett.* **88**(5), 051903 (2006).
- ¹¹M. Takeuchi, H. Shimizu, R. Kajitani, K. Kawasaki, T. Kinoshita, K. Takada, H. Murakami, Y. Kumagai, A. Koukitu, T. Koyama, S. F. Chichibu, and Y. Aoyagi, *J. Cryst. Growth* **305**(2), 360–365 (2007).
- ¹²J. Jasinski, Z. Liliental-Weber, Q. S. Padua, and D. W. Weyburne, *Appl. Phys. Lett.* **83**(14), 2811–2813 (2003).
- ¹³L. T. Romano, J. E. Northrup, and M. A. O'Keefe, *Appl. Phys. Lett.* **69**(16), 2394–2396 (1996).
- ¹⁴Y. Kumagai, J. Tajima, M. Ishizuki, T. Nagashima, H. Murakami, K. Takada, and A. Koukitu, *Appl. Phys. Express* **1**(4), 045003 (2008).
- ¹⁵S. Dasgupta, F. Wu, J. S. Speck, and U. K. Mishra, *Appl. Phys. Lett.* **94**(15), 151906 (2009).
- ¹⁶U. Haboeck, H. Siegle, A. Hoffmann, and C. Thomsen, *Phys. Status Solidi C* **0**(6), 1710–1731 (2003).
- ¹⁷A. R. Goni, H. Siegle, K. Syassen, C. Thomsen, and J. M. Wagner, *Phys. Rev. B* **64**, 035205 (2001).
- ¹⁸R. Kirste, S. Mohn, M. R. Wagner, J. S. Reparaz, and A. Hoffmann, *Appl. Phys. Lett.* **101**(4), 041909 (2012).
- ¹⁹K. B. Nam, J. Li, M. L. Nakarmi, J. Y. Lin, and H. X. Jiang, *Appl. Phys. Lett.* **82**(11), 1694–1696 (2003).
- ²⁰M. Feneberg, B. Neuschl, K. Thonke, R. Collazo, A. Rice, Z. Sitar, R. Dalmau, J. Xie, S. Mita, and R. Goldhahn, *Phys. Status Solidi A* **208**(7), 1520–1522 (2011).
- ²¹J. Li, K. B. Nam, M. L. Nakarmi, J. Y. Lin, H. X. Jiang, P. Carrier, and S.-H. Wei, *Appl. Phys. Lett.* **83**(25), 5163–5165 (2003).
- ²²B. N. Pantha, N. Nepal, T. M. A. Tahtamouni, M. L. Nakarmi, J. Li, J. Y. Lin, and H. X. Jiang, *Appl. Phys. Lett.* **91**(12), 121113–121117 (2007).
- ²³A. Sedhain, N. Nepal, M. L. Nakarmi, T. M. A. Tahtamouni, J. Y. Lin, H. X. Jiang, Z. Gu, and J. H. Edgar, *Appl. Phys. Lett.* **93**(4), 041903–041905 (2008).
- ²⁴R. Collazo, J. Xie, B. E. Gaddy, Z. Bryan, R. Kirste, M. Hoffmann, R. Dalmau, B. Moody, Y. Kumagai, T. Nagashima, Y. Kubota, T. Kinoshita, A. Koukitu, D. L. Irving, and Z. Sitar, *Appl. Phys. Lett.* **100**(19), 191914–191915 (2012).
- ²⁵R. Kirste, M. R. Wagner, J. H. Schulze, A. Strittmatter, R. Collazo, Z. Sitar, M. Alevli, N. Dietz, and A. Hoffmann, *Phys. Status Solidi A* **207**(10), 2351–2354 (2010).